Biomedicine & Pharmacotherapy 126 (2020) 110064

Contents lists available at ScienceDirect

Biomedicine & Pharmacotherapy

journal homepage: www.elsevier.com/locate/biopha

Chemopreventive role of arabinoxylan rice bran, MGN-3/Biobran, on liver carcinogenesis in rats

Nariman K. Badr El-Din[a,*], Doaa A. Ali[a], Reem Othman[a], Samuel W. French[b], Mamdooh Ghoneum[c]

[a] Department of Zoology, Faculty of Science, University of Mansoura, Mansoura, Egypt
[b] Department of Pathology and Laboratory Medicine, University of California, Los Angeles (UCLA), Los Angeles, CA, 90095, USA
[c] Department of Surgery, Charles Drew University of Medicine and Science, Los Angeles, CA, 90059, USA

ARTICLE INFO

Keywords:
Chemoprevention
Biobran
Hepatocarcinogenesis
Apoptosis
IkappaB-alpha

ABSTRACT

Hepatocellular carcinoma (HCC) is one of the most common cancers in the world and one of the most lethal. MGN-3/Biobran is a natural product derived from rice bran hemicelluloses and has been reported to possess a potent anticancer effect in a clinical study of patients with HCC. The current study examines the mechanisms by which Biobran protects against chemically induced hepatocarcinogenesis in rats. The chemical carcinogen used in this study is N-nitrosodiethylamine (NDEA) plus carbon tetrachloride (CCl_4). Rats were treated with this carcinogen, and the animals were pretreated or posttreated with Biobran via intraperitoneal injections until the end of the experiment. Treatment with Biobran resulted in: 1) significant alleviation of liver preneoplastic lesions towards normal hepatocellular architecture in association with inhibition of collagen fiber deposition; 2) arrest of cancer cells in the sub-G1 phase of the cell cycle; 3) increased DNA fragmentation in cancer cells; 4) down-regulated expression of Bcl-2 and up-regulated expression of p53, Bax, and caspase-3; and 5) protection against carcinogen-induced suppression of IkappaB-alpha (IκB-α) mRNA expression and inhibition of nuclear factor kappa-B (NF-κB/p65) expression. Additionally, the effect of Biobran treatment was found to be more significant when supplemented prior to carcinogen-induced hepatocarcinogenesis as compared to posttreatment. We conclude that Biobran inhibits hepatocarcinogenesis in rats by mechanisms that include induction of apoptosis, inhibition of inflammation, and suppression of cancer cell proliferation. Biobran may be a promising chemopreventive and chemotherapeutic agent for liver carcinogenesis.

1. Introduction

Liver cancer is a significant disease affecting a very large worldwide population; it is the ninth most commonly occurring cancer in women and the fifth most commonly occurring cancer in men, with over 840,000 new cases in 2018 [1]. Primary liver cancer, also called hepatocellular carcinoma (HCC), is the third leading cause of cancer mortality worldwide according to the World Health Organization (WHO) [2]. The most common treatments for HCC include chemotherapies such as doxorubicin, 5-fluorouracil, and cisplatin. However, liver cancer rarely responds well to whole-body chemotherapy and these drugs can only reduce a small portion of the tumor. New, safe, non-toxic agents that specifically target cancer cells are in high demand.

In a three-year clinical trial with HCC patients examining the combined effects of liver cancer drugs and the natural product Biobran, an extract of arabinoxylan rice bran [3], it was shown that combined treatment lowered disease recurrence, increased survival rate, and significantly lowered alpha-fetoprotein levels in comparison with patients treated with chemotherapy alone [4]. Biobran has long been examined for its various biological activities and has shown its potential as a non-toxic, anti-cancer agent. In mice studies, Biobran has been shown to exhibit anti-tumor activity against solid Ehrlich carcinoma tumor [5] and neuroblastoma [6], to enhance radiation therapy-induced tumor regression [7], and to augment the apoptotic effect of a low dose of paclitaxel on tumor cells [8], and in rat studies, Biobran has been shown to provide protection against chemically induced glandular stomach carcinogenesis [9]. The mechanisms by which Biobran exerts anti-cancer effects have been attributed to its ability to act as a potent biological response modifier (BRM) that activates different arms of the immune system, including activating dendritic cells (DCs) [10–12] and natural killer (NK) cells [5,13–17], increasing human T and B cell

* Corresponding author at: Department of Zoology, Faculty of Science, University of Mansoura, Mansoura, 35516, Egypt.
E-mail address: na_ri_eg@yahoo.com (N.K. Badr El-Din).

https://doi.org/10.1016/j.biopha.2020.110064
Received 4 February 2020; Received in revised form 26 February 2020; Accepted 28 February 2020

mitogen responses [3], and augmenting phagocytosis by macrophages [18].

In a previous preliminary study, we showed that Biobran exerts a protective effect against hepatocarcinogenesis induced by N-nitrosodiethylamine (NDEA) plus carbon tetrachloride (CCl_4) in rats, specifically by showing that Biobran reverses the negative effects of this carcinogen on body weight, liver weight, and liver enzyme levels [19]. In the current study, we aimed to examine the specific mechanisms behind Biobran's protective effect on chemically induced hepatocarcinogenesis in rats. Specifically, we focused on the ability of Biobran to induce a potent apoptotic effect against liver cancer cells as a primary underlying molecular mechanism, and we evaluated its anti-inflammatory effect on the expression of IkB-α mRNA and subsequent inhibition of NF-κB signaling.

2. Materials and methods

2.1. MGN-3/Biobran

Biobran is a polysaccharide made up of β1,3-glucan and activated hemicellulose. This product is obtained from rice bran treated enzymatically with a Shiitake mushroom extract. Biobran was freshly prepared by dissolving it in 0.9 % saline and injecting the solution into rats intraperitoneally (i.p.) at a dose of 25 mg/kg-body-weight/day five times/week via a single 0.2 ml shot. Biobran was provided by Daiwa Pharmaceuticals Co., Ltd., Tokyo, Japan.

2.2. Animals

In the current study, we used 90 male Wistar rats, aged 4 months (~120 g body weight). The animals were obtained from the Research Institute of Ophthalmology (Giza, Egypt) and acclimatized for one week prior to the commencement of the study. Rats were caged individually with light and temperature controls (20 ± 2 °C) and were fed standard laboratory cube pellets. The animal treatments described in this study were reviewed and approved by the Mansoura University Animal Care and Use Committee.

2.3. Induction of hepatocarcinogenesis

A single dose of the carcinogenic compound N-nitrosodiethylamine (NDEA) (200 mg/kg body weight) was administered via i.p. injection to rats. After one week, animals received weekly subcutaneous (s.c.) injections of carbon tetrachloride (CCl_4) (3 ml/kg body weight) for 6 weeks [20]. NDEA was obtained from Sigma Chemical Company, USA; CCl_4 was obtained from El-Gomhorya Co., Cairo, Egypt.

2.4. Experimental design

The 90 rats were randomly assigned into five experimental groups. Group 1 was the control untreated group (15 rats). Group 2 received only Biobran by i.p. injection (25 mg/kg-body-weight/day) five times/week (15 rats). Group 3 received only the carcinogen (NDEA + CCl_4) (20 rats). Group 4 received Biobran (25 mg/kg-body-weight/day) five times/week beginning 2 weeks prior to carcinogen injection and continuing for 20 weeks (20 rats). Group 5 received Biobran (25 mg/kg-body-weight/day) five times/week starting at week 10 after carcinogen injection and continuing until the end of the study (20 rats). These timelines are depicted in Fig. 1. Body weight was monitored throughout the length of the experiment (data not shown).

2.5. Sample collections

After 22 weeks of experimental study, the animals were allowed to fast before being anesthetized using diethyl ether. Animals were weighed and then dissected. Their livers were obtained, washed in ice cold saline, patted dry, and weighed. Liver specimens were obtained from each rat for measuring the different parameters. Parameters under investigation in liver tissues included histopathology, flow cytometric analysis of cell cycle progression, apoptosis, apoptotic and cell proliferation protein regulators (p53, Bax, Bcl-2, caspase-3, and NF-κB/p65 expression), and reverse transcription-polymerase chain reaction (RT-PCR) to determine relative gene expression of p53, Bax, Bcl-2, caspase-3, and IκB-α. DNA damage was detected by gel electrophoresis, in addition to the detection of NF-κB/p65 expression by immunostaining.

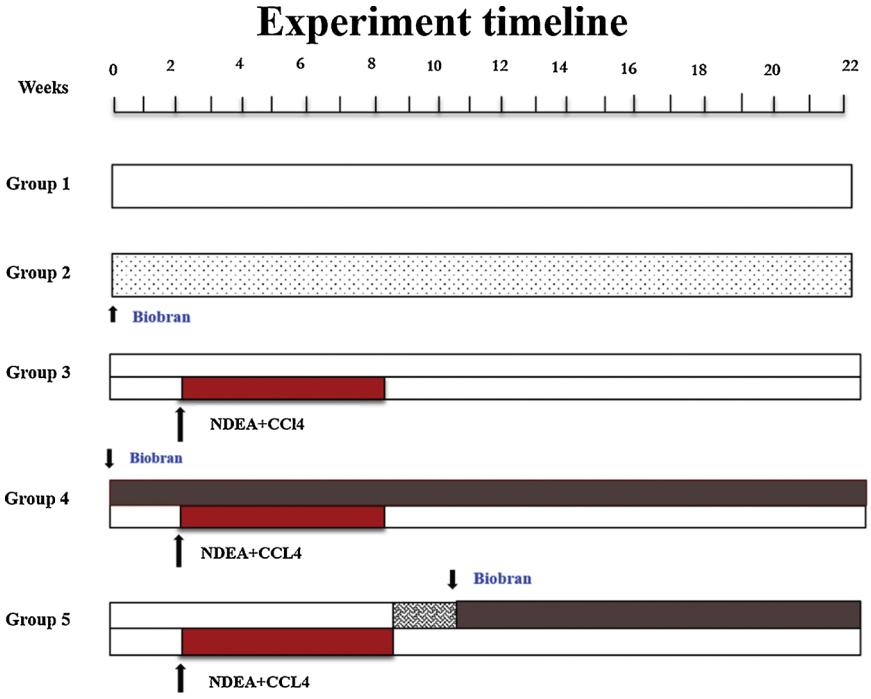

Fig. 1. Schematic presentation of the experimental regimen.

2.6. Histopathology

For histological processing, liver specimens of the different groups were collected. Tissues were cut into small pieces and immediately fixed in 10 % neutral buffer formalin for 24 h. After fixation, specimens were dehydrated in ascending series of ethyl alcohol 70 %–95 % followed by two changes of absolute ethyl alcohol. Tissues were cleared in xylene and then embedded in paraffin wax. Sections 4 to 5 μm thick were cut using a microtome, mounted on glass slides, and stained by H& E for histopathology and Masson's trichrome method for collagen fibers [21].

2.7. Flow cytometric studies: liver cells preparation

Tissue samples were excised from livers of the different groups, cut into pieces, and rubbed gently through fine nylon gauze (40–50 mesh count/cm; HD 140 Zuricher Buteltuchfabrik AG, Zürich, Switzerland). Samples were washed through the gauze with Tris-ethylene diamine tetraacetic acid (Tris-EDTA) buffer at pH 7.5 [3.029 g of 0.1 M Tris-(hydroxymethyl aminomethane), 1.022 g of 0.07 M HCl, and 0.47 g of 0.005 M Tris-EDTA]. Cells were suspended in sterile PBS, centrifuged for 10 min at 1800 rpm, resuspended in PBS (cell density $\sim 1 \times 10^4$ cells/ml) and fixed in 70 % ice cold ethanol mixed with PBS and stored at -20 °C until analyzed.

2.8. Cell cycle analysis

Liver cell suspensions were centrifuged and cell pellets were re-suspended in 1 ml of propidium iodide (PI) solution and incubated for 30 min in the dark. Subsequent assays were performed using flow cytometry. Data analysis was conducted using the DNA analysis program MODFIT (Verity Software House, Inc., Topsham, ME, USA). For each sample, the software calculated the coefficient of variation around the G0/G1 peak and the percentage of cells in each phase (G0/G1, S, and G2/M) of the DNA cell cycle. If a distinct peak separate from the G1 diploid peak deviated by over 10 % from the diploid internal standard, or if the G1 peak deviated from a corresponding G2/M peak by more than 10 %, then an aneuploid cell population was classified as present [22].

2.9. Quantitative determination of apoptotic cell death

Induction of apoptosis caused by Biobran treatment in liver cancer cells was quantitatively determined through flow cytometry using the Annexin-V-conjugated Alexafluor 488 Apoptosis Detection Kit following the manufacturer's instructions (BD Biosciences, San Jose, CA). The early apoptotic cells stained with Alexa488 fluoresce green and present in the lower right quadrant of the fluorescence-activated cell-sorting histogram, and the late apoptotic cells stained with both Alexa488 and propidium iodide fluoresce red-green and present in the upper right quadrant of the fluorescence-activated cell-sorting histogram.

2.10. Flow cytometric analysis of apoptotic regulators

Analysis of apoptosis related protein mouse antibodies against p53 (sc-7480), Bax (sc-7480), Bcl-2 (sc7382), caspase-3 (sc-7272), and NF-κB/p65 (sc-8008) and other reagents were purchased from Santa Cruz Biotechnology, Inc., Dallas, TX, USA. Secondary antibodies were available as fluorescein [fluorescein isothiocyanate (FITC)] conjugates for flow cytometry. Normal and tumor cells (1×10^6) from the different groups were incubated with the appropriate antibody for 1 h at room temperature followed by FITC conjugated goat-anti-rabbit antibody. Cells were washed thoroughly with phosphate-buffered saline and bovine serum albumin and analyzed on a flow cytometer (Becton Dickinson, San Jose, CA, USA). A total of 20,000 cells were acquired for analysis by CellQuest software, and histogram plots of FITC-fluorescence vs counts in logarithmic fluorescence intensity were used to obtain mean values.

2.11. Real-time RT-PCR analysis of apoptotic regulators and IκB-α gene expression

RT-PCR analysis of apoptotic regulators was performed following the manufacturer's instructions, and total RNA extraction was performed using a GF-TR-050 Total RNA Extraction Kit (Vivantis Technologies SDN. BHD., Malaysia). The total RNA was reverse transcribed into cDNA using FastQuant RT Kit (Tiangen Biotech (Beijing) Co., Ltd). The kit contained gDNase that removed genomic DNA by incubation at 42 °C for 3 min to protect the total RNA analysis from genomic DNA interference. RT-PCR was performed using Maxima SYBR Green qPCR Master Mix (2×) Kit (Thermo Scientific). Reaction conditions and data analysis were used per the manufacturer's instructions: 5 μl of cDNA in a total volume of 25 μl containing 12.5 μl Maxima SYBR Green qPCR Master Mix (2×), 0.3 μMol forward primer, 0.3 μMol reverse primer (primers are shown in Table 1), and 10 nM/100nM ROX Solution and brought up to 25 μl with nuclease-free water. Thermal cycling conditions were 95 °C for 10 min, followed by 40 cycles of 95 °C for 15 s, 58 °C for 30 s, and 60 °C for 30 s. Reactions were run with a PIKO REAL 96 Real-Time PCR system (Thermo Scientific). Differences in gene expression between groups were determined using the ΔΔC cycle time (Ct) method [23] and were normalized against the glyceraldehyde-3-phosphate dehydrogenase (GAPDH) house-keeping gene. Data were expressed as relative mRNA levels as compared with the level of the normal control group.

2.12. Detection of DNA damage by gel electrophoresis

DNA extraction of liver tissues was performed using a TIANamp Genomic DNA Kit (TIANGEN Biotech (Beijing) Co., Ltd) following the manufacturer's instructions. Standard gel electrophoresis in an agarose gel was used to separate DNA by size (e.g., length in base pairs) in order to visualize and purify DNA samples. The length of a DNA segment was determined using a DNA ladder. After running, the gel was analyzed by Gel Analyzer Pro v3.1 which automatically detected lanes and bands.

2.13. Immunohistochemical detection of NF-κB/p65 expression

Sections of liver tissues were cut onto positive-charged slides and incubated with mouse monoclonal anti-NF-κB/p65 antibody (sc-8008) purchased from Santa Cruz Biotechnology, Inc. (Dallas, TX, USA). Immunohistochemical staining was performed using the streptoavidine-biotin method with a Histostain-plus kit (Santa Cruz Biotechnology) containing 10 % non-immune serum, biotinylated secondary antibody, and streptoavidine-peroxidase. DAB was used as a chromogen and Mayer's Hematoxylin was applied as a counterstain to sections. The slides were then observed by light microscopy. Expression of NF-κB/p65 was detected in the cytoplasm of liver tissues. Positive NF-κB signals appeared brown. Any sections with < 5% positive cells were recorded as negative.

2.14. Statistical analysis

Data are reported as mean ± standard error (SE) of measurement. Statistical significance was determined by one-way ANOVA followed by the post-hoc LSD test for analyzing statistically significant differences between groups. The analysis was carried out using the Statistical Package for the Social Sciences (SPSS) software version 16. Differences were considered significant at the $p < 0.05$ level.

Table 1
Sequence of primers used for RT-PCR. IκB-α, p53, Bcl-2, and GAPDH are designed by (VIVANTIS, MALISYA), caspase-3 and Bax by (METABION, GERMANY).

Gene	Forward primer	Reverse primer
IκB-α	5-CCCAAGTACCCGGATACAGC-3	5-GGGCAACTCATCTTCCGTGA-3
p53	5-AGTTAGGGGGTACCTGGCAT -3	5-GACTCAGAGGGAGCTCGATG -3
caspase-3	5-GGAGCTTGGAACGCGAAGAA -3	5-CAGAGTCCATCGACTTGCTTCC -3
Bax	5-ATG CTC CAC CAA GAA GCT GA-3	5-AGC AAT CAT CCT CTG CAG CTC C-3
Bcl-2	5-ATCGCTCTGTGGATGACTGAGTAC -3	5-AGAGACAGCCAGGAGAAATCAAAC -3
GAPDH	5-TTGTGCAGTGCCAGCCTCGT -3	5-TGCCGTTGAACTTGCCGTGG -3

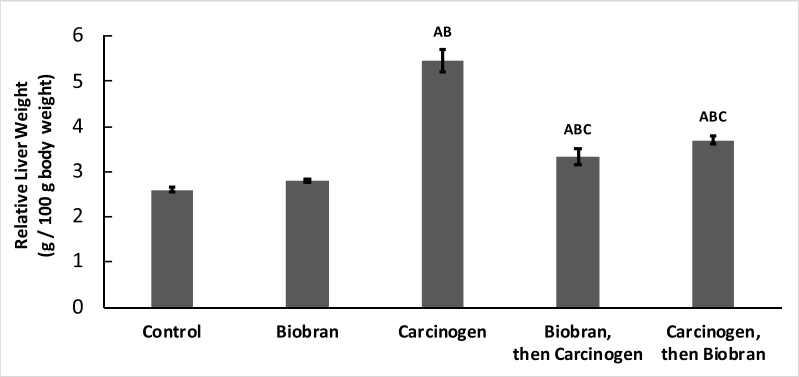

Fig. 2. Relative liver weight. Each value represents the mean ± SE of the corresponding number of animals/group: Control (13), Biobran alone (13), Carcinogen (15), Biobran then Carcinogen (18), Carcinogen then Biobran (17).
[A] Significantly different from Control group at $p < 0.01$ level.
[B] Significantly different from Biobran group at $p < 0.01$ level.
[C] Significantly different from Carcinogen group at $p < 0.01$ level.

3. Results

3.1. Relative liver weight (RLW)

Rats exposed to the carcinogen (NDEA plus CCl_4) demonstrated a significant increase in RLW compared to controls. However, treatment with Biobran either before or after exposure to the carcinogen normalized the increase in RLW to be within the normal control values (Fig. 2).

3.2. Cell cycle progression and apoptosis

The effects of the carcinogen and of Biobran on the different phases of the cell cycle in normal and tumor liver cells was examined. Data in Table 2 show that Biobran treatment in the presence of the carcinogen caused cell-cycle arrest in the sub-G1 phase, where the hypodiploid cell population was markedly increased by 126 % and 99 % ($p < 0.01$) for pretreatment and posttreatment, respectively, as compared to the group treated with the carcinogen alone. Administration of Biobran to the carcinogen group caused disruption of the tumor cell cycle status (G0/G1, S, and G2/M phases) with no cell cycle arrest.

3.3. Quantitative determination of apoptosis by AnnexinV/PI staining

Data in Table 3 shows that Biobran pretreatment or posttreatment to the carcinogen significantly ($p < 0.01$) increased the early apoptotic population by 316 % and 309 %, respectively, when compared to the untreated carcinogen group. The percentage of the late apoptotic cell population recorded a marked increase ($p < 0.01$) of 237 % for the Carcinogen + Biobran group, while pretreatment with Biobran (Biobran + Carcinogen) recorded a larger increase (255 %, $p < 0.01$) as compared with the late apoptotic cell population of the untreated carcinogen group.

3.4. Flow cytometric analysis of apoptotic regulators

Effects of carcinogen and Biobran on the percentage of apoptotic regulators' expression in the livers' normal and tumor cells were examined by flow cytometry. Results in Table 4 show that Biobran induced apoptosis in liver cancer cells *in vivo* via the mitochondria-dependent pathway and that effects of pretreatment were more marked versus posttreatment, as indicated by a 107 % versus 77 % increase in p53 expression, a 129 % versus 108 % increase in Bax expression, a 48 % versus 51 % decrease in Bcl-2 expression, a 335 % versus 333 %

Table 2
Cell cycle progression and apoptosis in liver tissue of the different groups. Each value represents the mean ± SE of 6 rats/group.

Groups Parameter	Control	Biobran	Carcinogen	Biobran, then Carcinogen	Carcinogen, then Biobran
Sub G1 (M1)	6.77 ± 0.49	9.34 ± 0.95	37.55 ± 1.42^{AB}	85 ± 1.21^{ABC}	74.75 ± 1.46 ^{ABC}
% change from Carcinogen	–	–	–	126 %	99 %
G0/G1 (M2)	55 ± 2.85	56.18 ± 3.36	34.5 ± 1.83^{AB}	12.77 ± 1.62^{ABC}	16.33 ± 3.65^{ABC}
% change from Carcinogen	–	–	–	−62.94 %	−52.64 %
S phase (M3)	16.31 ± 1.63	14.18 ± 1.94	12.62 ± 2.55	1.48 ± 0.16^{ABC}	5.69 ± 1.67^{ABCD}
% change from Carcinogen	–	–	–	−88.27 %	−54.94 %
G2/M (M4)	18.58 ± 2.72	16.17 ± 1.76	5.56 ± 1.12^{AB}	1.73 ± 1.69^{ABC}	3.56 ± 0.54^{ABc}
% change from Carcinogen	–	–	–	−68.90 %	−35.85 %

[A]Significantly different from the Control group at $p < 0.01$ level.
[B] Significantly different from the Biobran group at $p < 0.01$ level.
[C]Significantly different from the Carcinogen group at $p < 0.05$ and $p < 0.01$ levels.
[D] Significantly different from the Biobran + Carcinogen group at $p < 0.01$ level.

Table 3
Flow cytometric analysis of apoptosis by Annexin V/PI double staining in the liver tissue of the different groups. Each value represents the mean ± SE of 6 rats/group.

Groups Parameter	Control	Biobran	Carcinogen	Biobran, then Carcinogen	Carcinogen, then Biobran
Viable cells	**96 ± 1.45**	**91 ± 0.30**	**77.25 ± 2.54^{AB}**	**18.86 ± 1.40^{ABC}**	**20.32 ± 1.58^{ABC}**
% change from Carcinogen group	–	–	–	**−74.51%**	**−72.54 %**
Early apoptosis	**2 ± 0.41**	**3.42 ± 0.22**	**7.67 ± 1.36^{AB}**	**32.9 ± 2.27^{ABC}**	**31 ± 2.83^{ABC}**
% change from Carcinogen group	–	–	–	316 %	309 %
Late apoptosis	**2.37 ± 0.63**	**6.16 ± 0.57**	**13.92 ± 1.55^{AB}**	**49 ± 1.86^{ABC}**	**47 ± 2.52^{ABC}**
% change from Carcinogen group	–	–	–	255 %	237 %
Necrosis	**0.43 ± 0.73**	**0.19 ± 0.21**	**3.18 ± 0.08^{AB}**	**0.78 ± 1.17^{ABC}**	**0.35 ± 0.19^{aBCD}**
% change from Carcinogen group	–	–	–	**−89 %**	**−75.47 %**

[A] Significantly different from the Control group at $p < 0.01$ level.
[B] Significantly different from the Biobran group at $p < 0.01$ level.
[C] Significantly different from the Carcinogen group at $p < 0.01$ level.

increase in Bax/Bcl-2 ratio, and a 66 % versus 51 % increase in caspase-3 activity for pretreatment and posttreatment, respectively, as compared with carcinogen-untreated rats.

3.5. Relative gene expression of apoptotic regulators

Effects of carcinogen and Biobran on the percentage of relative gene expression of apoptotic regulators in the liver tissues of the different groups were examined by RT-PCR technique. As shown in Table 5, the untreated carcinogen group showed low levels in p53, Bax, and caspase-3 gene expression and high levels of Bcl-2 gene expression. Pretreatment by Biobran significantly ($p < 0.01$) upregulated p53, Bax, and caspase-3 gene expression by +143 %, +80 %, and +96.71 %, respectively, and downregulated Bcl-2 gene expression levels by −53 % as compared to that of the untreated carcinogen group. Similarly, but to a lower extent, Biobran posttreatment showed marked upregulation ($p < 0.01$) for p53, Bax, and caspase-3 gene expression and marked downregulation in Bcl-2 gene expression versus the untreated carcinogen group.

3.6. Flow cytometric and immunohistochemical detection of NF-κB/p65 expression

Flow cytometric detection showed a marked downregulation of NF-κB/p65 protein levels in liver cells of pretreated and posttreated Biobran-carcinogen groups by −46.08 % and −38.87 %, respectively, relative to the untreated carcinogen group (Fig. 3A). Results of the histochemical analysis of immunoreactivity in the liver tissues of both control and Biobran treated rats showed negative expression of NF-κB/p65 in the cytoplasm of the hepatic cells. Liver tissues of carcinogen treated rats expressed strong cytoplasmic NF-κB/p65 immunoreactivity localized at the area of inflammation and fibrosis. Biobran treatment decreased the cytoplasmic NF-κB/p65 expression to show weak positive immunoreactivity in a small number of liver cells for pretreatment and mild positive expression for posttreatment (Fig. 3B).

3.7. Relative gene expression of IκB-α

Quantitative determination of IκB-α gene expression in liver tissues of the different groups by the RT-PCR technique are shown in Fig. 4. Animals treated with Biobran alone showed no significant change in the gene expression of IκB-α gene as compared to normal control animals. Injection of carcinogen to rats significantly ($p < 0.01$) decreased the level of IκB-α gene expression to 0.53 ± 0.03. Administration of Biobran 2 weeks before the injection of carcinogen and throughout the experimental period reversed the decrease of IκB-α gene expression to record a marked upregulation by 131 % when compared with the untreated carcinogen group. Meanwhile, posttreatment with Biobran prevented the suppression of the gene expression level of IκB-α induced by the carcinogen to record an elevation by 76.57 % as compared to the untreated carcinogen group.

3.8. Detection of DNA damage by gel electrophoresis

Nuclear DNA fragmentation, a characteristic hall-mark of apoptosis, was investigated in the liver tissues of the different groups by gel electrophoresis and analyzed by Image J software. DNA agarose electrophoresis is a highly specific method of detecting apoptosis, with the demonstration of characteristic ladders of DNA signifying apoptosis. As shown in Fig. 5, the DNA fragmentation in liver cells of the untreated

Table 4
Flow cytometric analysis of apoptotic regulators in the liver tissues of the different groups. Each value represents the mean ± SE of 6 liver samples/group.

Groups Parameter	Control	Biobran	Carcinogen	Biobran, then Carcinogen	Carcinogen, then Biobran
p53	**5.19 ± 0.31**	**6.37 ± 0.35**	**14.54 ± 0.52^{AB}**	**30 ± 1.3^{ABC}**	**26 ± 0.92^{ABCD}**
% change from Carcinogen group	–	–	–	107.36 %	76.97 %
Bax	**10.85 ± 0.48**	**9.57 ± 0.85**	**20.69 ± 1.14^{AB}**	**47 ± 1.73^{ABC}**	**43.61 ± 2.52^{ABC}**
% change from Carcinogen group	–	–	–	129 %	108.25 %
Bcl-2	**15.59 ± 1.15**	**14.50 ± 1.11**	**64 ± 2.08^{AB}**	**34 ± 1.33^{ABC}**	**31.18 ± 0.75^{ABC}**
% change from Carcinogen group	–	–	–	**−48 %**	**−51.31 %**
Bax/Bcl-2 ratio	**0.697 ± 0.06**	**0.665 ± 0.1**	**0.323 ± 0.02^{AB}**	**1.406 ± 0.05^{ABC}**	**1.399 ± 0.11^{ABC}**
% change from Carcinogen group	–	–	–	335 %	332.6 %
Caspase-3	**7.92 ± 0.64**	**10.43 ± 0.44**	**22.85 ± 1.29^{AB}**	**38 ± 1.14^{ABC}**	**34.57 ± 1.06^{ABC}**
% change from Carcinogen group			–	66.43 %	51.29 %

[A] Significantly different from the Control group at $p \leq 0.01$ level.
[B] Significantly different from the Biobran group at $p \leq 0.01$ level.
[C] Significantly different from the Carcinogen group at $p \leq 0.01$ level.
[D] Significantly different from the Biobran + Carcinogen group at $p \leq 0.01$ level.

Table 5
Effects of different treatments on relative gene expression of p53, Bax, Bcl-2, and caspase-3 in liver tissues of rats as determined by RT-PCR. Relative gene expression was quantified with GAPDH as an internal control. Data are represented as % increase or decrease relative to the levels of the control group. The relative gene expression of the normal control group is defined as 1. Each value represents the mean ± SE of 5 liver samples/group.

Groups Parameter	Control	Biobran	Carcinogen	Biobran, then Carcinogen	Carcinogen, then Biobran
p53 gene	**1**	**0.99 ± 0.07**	**0.65 ± 0.03^{AB}**	**1.59 ± 0.09^{ABC}**	**1.27 ± 0.15 ^{abCd}**
% change from Carcinogen group	–	–	–	+143 %	+94 %
Bax gene	**1**	**1.06 ± 0.05**	**0.67 ± 0.09^{AB}**	**1.21 ± 0.12^{ABC}**	**0.97 ± 0.07 ^{Cd}**
% change from Carcinogen group	–	–	–	80 %	44 %
Bcl-2 gene	**1**	**1.13 ± 0.18**	**4.21 ± 0.48^{AB}**	**1.99 ± 1.25^{ABC}**	**2.30 ± 1.6^{ABC}**
% change from Carcinogen group	–	–	–	**−53 %**	**−45.32 %**
caspase-3 gene	**1**	**0.99 ± 0.06**	**0.85 ± 0.09^{ab}**	**1.67 ± 0.25^{ABC}**	**1.36 ± 0.12^{abC}**
% change from Carcinogen group	–	–	–	+96.71 %	+60.24 %

[a,A] Significantly different from the Control group at $p < 0.05$, $p < 0.01$ levels, respectively.
[b,B] Significantly different from the Biobran group at $p < 0.05$, $p < 0.01$ levels, respectively.
[c,C] Significantly different from the Carcinogen group at $p < 0.05$, $p < 0.01$ levels, respectively.
[d] Significantly different from the Biobran + Carcinogen group at $p < 0.05$ level.

carcinogen group produced an OD percentage of 13.36 ± 3.82 and showed no ladder formation. In contrast, the broken DNA strands in the liver cells of the Biobran posttreatment group recorded an OD percentage of 62.10 ± 7.94 (+364.83 % of the carcinogen group). Pretreatment with Biobran to rats exposed to carcinogen showed more DNA damage and recorded the highest percentage of DNA laddering (% OD = 77.14 ± 4.50), measuring +477.35 % of the untreated carcinogen group.

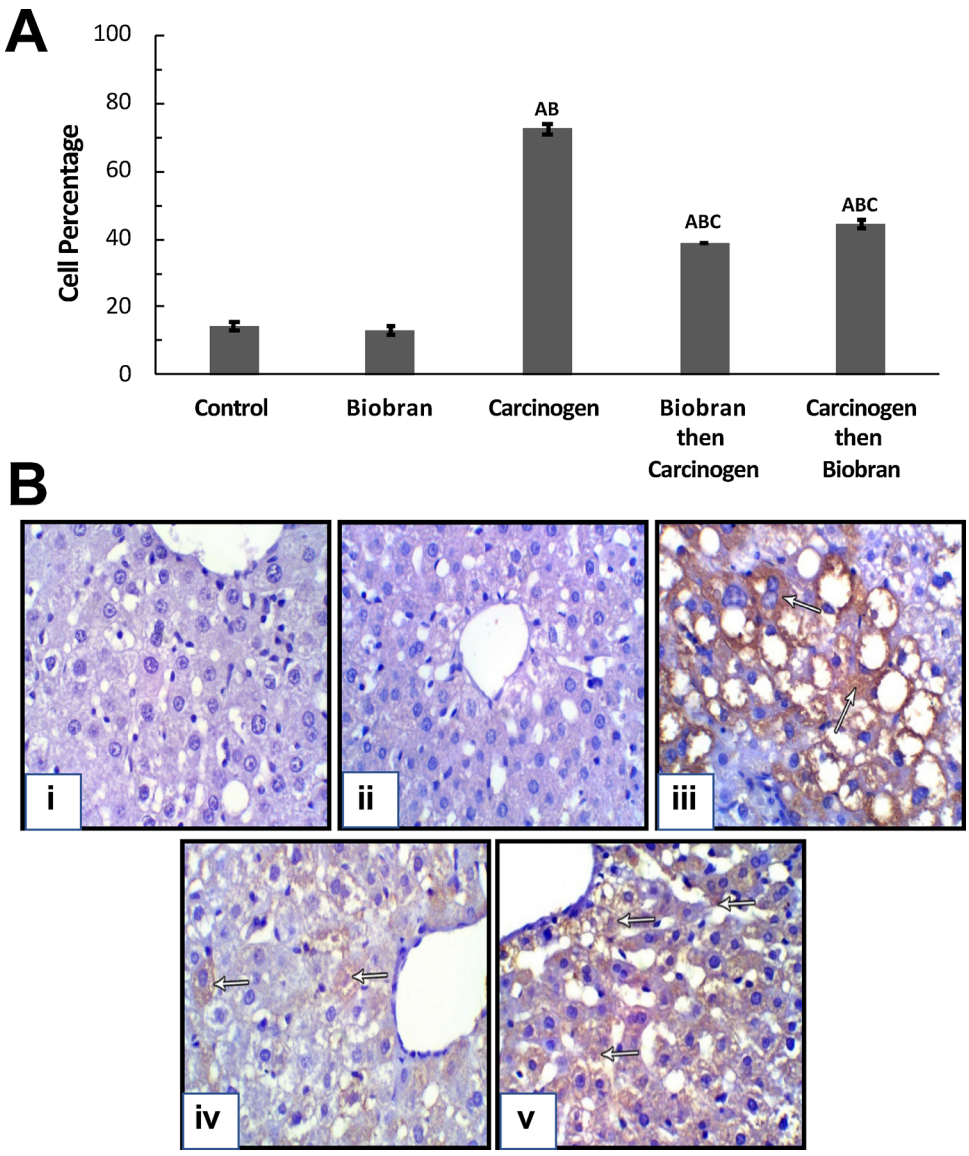

Fig. 3. (A) Flow cytometric determination of NF-κB/p65 expression in the liver tissues of the different groups. Each value represents the mean ± SE of 6 liver samples/group. (B) Immunohistochemical examination of NF-κB/p65 expression in liver tissues. (i) Negative cytoplasmic immunostaining in the normal Control group. (ii) Negative cytoplasmic immunostaining in the Biobran group. (iii) Strong dark brown cytoplasmic immunoreactivity in the tumor cells of Carcinogen group. (iv) Weak positive cytoplasmic expression in some tumor cells of pretreated group. (v) Mild cytoplasmic immunopositivity in some tumor cells of post-treated group (A-E, 400X).
[A] Significantly different from Control group at $p < 0.01$ level.
[B] Significantly different from Biobran group at $p < 0.01$ level.
[C] Significantly different from Carcinogen group at $p < 0.01$ levels.

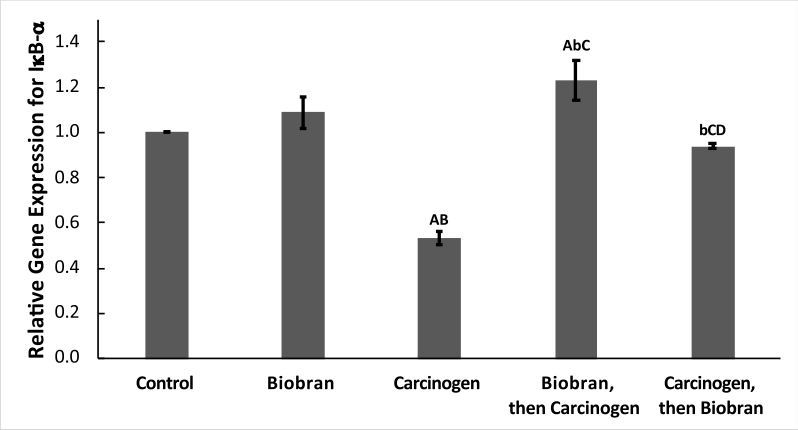

Fig. 4. Effect of different treatments on relative gene expression of IκB-α in liver tissues of rats as determined by RT-PCR. Each value represents the mean ± SE of 5 tumor samples/group.
[a,A] Significantly different from Control group at $p < 0.05$, $p < 0.01$ levels, respectively.
[b,B] Significantly different from Biobran group at $p < 0.05$, $p < 0.01$ levels, respectively.
[c,C] Significantly different from Carcinogen group at $p < 0.05$, $p < 0.01$ levels, respectively.
[d] Significantly different from Biobran then Carcinogen group at $p < 0.05$ level.

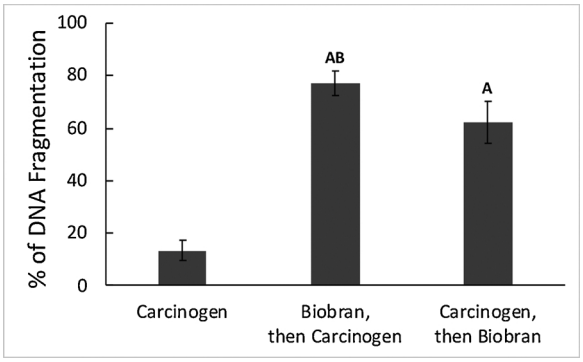

Fig. 5. % of DNA fragmentation obtained by gel electrophoresis in liver tissues of rats analyzed by Image J software. Data express the mean ± SE of 3 different gel electrophoresis runs.
[A] Significantly different from Carcinogen group at $p < 0.01$ level.
[B] Significantly different from Carcinogen then Biobran group at $p < 0.01$ level.

3.9. Liver pathology

The carcinogen induced different proliferative and preneoplastic lesions in the livers of rats. Data of liver pathology are shown in Fig. 6 (left vertical panel, A-E). Normal control liver shows no abnormality (A). Liver sections of Biobran treated rats showed normal liver structure (B). Treatment with carcinogen revealed loss of liver architecture with the formation of hyperplastic nodules separated by fibrous septa with invasive inflammatory cells and bile duct proliferation. Carcinogen treatment caused steatosis. Features included large and small droplet macrovesicular steatosis with no zonal distribution, focal hepatocellular cytoplasmic clearing, polymorphism of nuclei, and frequent mitotic activity (C). Treatment with Biobran prior to nitrosamine injection showed no appearance of steatosis and preserved hepatic architecture with minimal nuclear changes and inflammation (D). Treatment with Biobran post nitrosamine injection decreased the appearance of steatosis and showed few lipid droplets (LD), as well as showing moderate portal inflammatory infiltrates (mostly lymphocytes) and few degenerated hepatocytes (E).

3.10. Histological observation of collagen fibers in liver tissue

Data in Fig. 6 (right vertical panel, F-J) shows the histopathological observation of collagen fibers in liver tissue. Liver sections of control animals (F) and Biobran control animals (G) showed negligible amounts of collagen fibers around the central vein and slight fibrous septa between the hepatic cells. On the other hand, liver sections of carcinogen treated rats showed a severe deposition of collagen fibers surrounding the hyperplastic nodules pseudolobules, which resulted in severe fibrosis that distorted the hepatic architecture (H). On the other hand, liver tissues of animals pretreated with Biobran before the carcinogen displayed slight deposition of collagen fibers around the central vein, indicating that Biobran protected the liver from progressive fibrosis (I). Animals posttreated with Biobran also showed a moderate amount of collagen fibers around the congested central when compared with carcinogen treated animals (J).

4. Discussion

Previous clinical studies with hepatocellular carcinoma (HCC) patients have shown that MGN-3/Biobran synergizes with conventional therapies (CT) and results in greater reduction in tumor size, less recurrence of cancer, and higher survival rate as compared with patients treated with CT alone [4]. In our previous preliminary studies in which liver cancer was induced in rats by a carcinogen (NDEA plus CCl_4), rats had a marked decrease in body weight and increase in liver weight and liver enzyme levels, but rats treated with Biobran were found to maintain normal body weight, liver weight, and liver enzyme levels [19]. In the current study, we investigated the underlying mechanisms of Biobran's activity by studying the induction of apoptosis and inhibition of inflammation and cancer cell proliferation, as well as by performing molecular studies of gene and protein expression and DNA fragmentation.

With regard to apoptosis, we examined the cell cycle and apoptotic regulators in order to gain insight into the underlying protective mechanisms of Biobran against chemically induced liver carcinogenesis. Biobran induced apoptosis in liver cancer cells via cell-cycle arrest of liver cancer cells in the sub-G1 phase, where apoptosis was evidenced by a marked increase in the hypodiploid cell population. Flow cytometry using Annexin V/PI double staining showed an increase in the levels of early and late apoptosis in the liver cancer cells, as well as a significant inhibition in the viable cell count. These data agree with previous Biobran studies showing an apoptotic mechanism for solid tumor regression in mice [5,8] and for gastric cancer cells in rats [9]. We further studied apoptosis with a nuclear DNA fragmentation based approach, where apoptosis was investigated by DNA gel electrophoresis. The DNA damage of rats treated with Biobran showed the highest degree of DNA laddering as compared with the carcinogen group. A DNA ladder pattern is known to confirm a high apoptosis rate [24]. These data agree with previous studies showing a decrease in cell proliferation and increases in DNA damage and apoptosis in solid tumors of mice treated with Biobran, either alone or in combination with chemotherapy [8].

The exact mechanism by which Biobran exerts its apoptotic effect could be related to the ability of Biobran to sensitize the surface CD95 receptors that are involved in the triggering of apoptosis [25] or via a mitochondrial dependent pathway. The indication in our current study

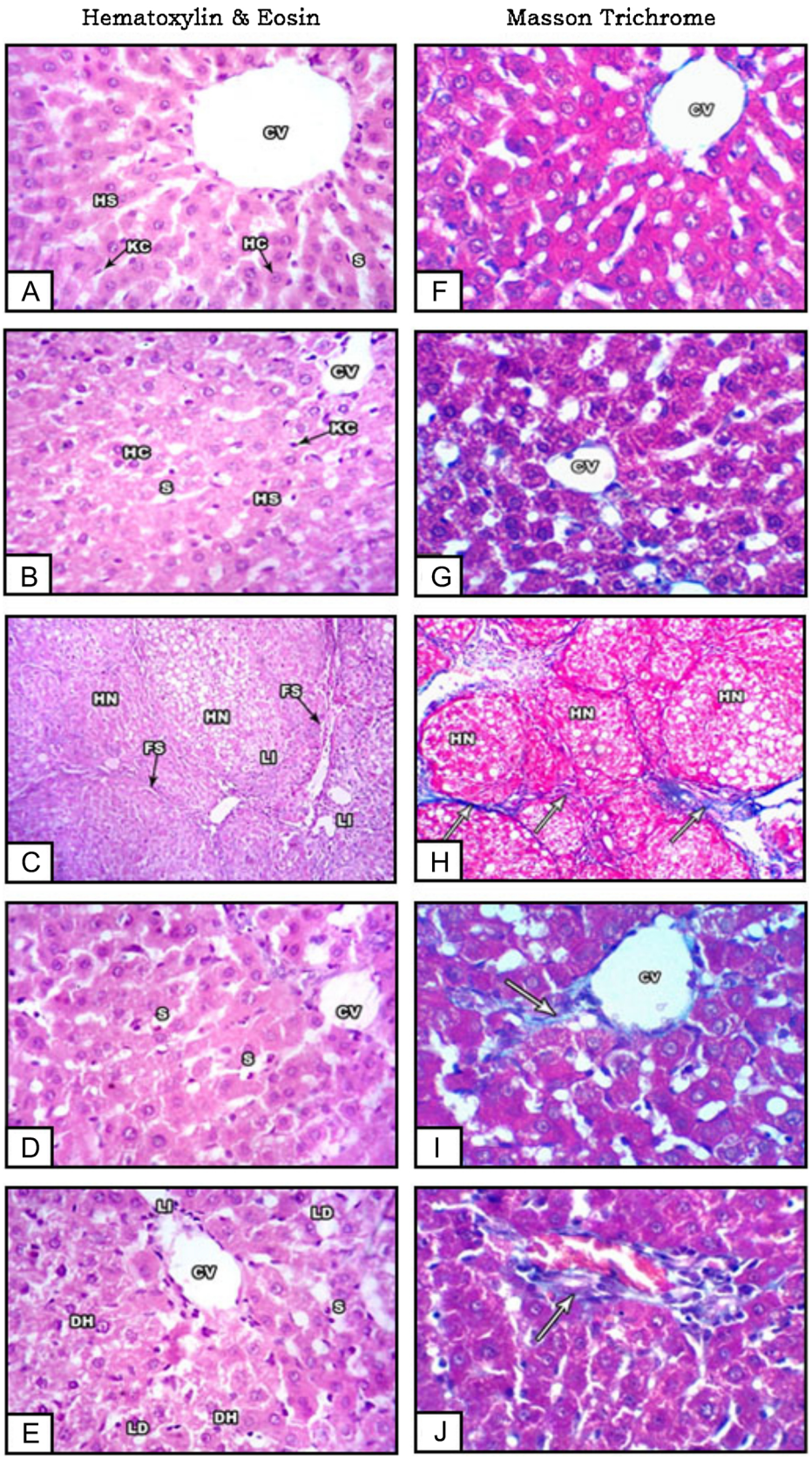

Fig. 6. Left vertical panel represents representative photomicrographs of liver sections stained with H& E: (A) Normal control liver shows no abnormality (x400). (B) Liver sections of Biobran treated rats showed normal liver structure (x400). (C) Treatment with carcinogen revealed loss of liver architecture, hyperplastic nodules (HN) separated with intense fibrous septa (FS) with leucocyte infiltration (LI), large amounts of steatotic foci comprised of variably mixed micro and macrovesicular steatosis in the cytoplasm, and an increase in mitotic activity (x100). (D) Treatment with Biobran prior to carcinogen injection preserved the hepatic architecture, showed no steatosis, and minimized the nuclear changes and vacuolation of hepatocellular cytoplasm (x400). (E) Treatment with Biobran post carcinogen injection decreased the appearance of steatosis and showed few lipid droplets (LD), moderate portal inflammatory infiltrates, and few degenerated hepatocytes (DH) (x400). Right vertical panel represents representative photomicrographs of liver sections stained with Masson trichrome. (F) Normal control liver shows negligible amounts of collagen fibers (x400). (G) Liver sections of Biobran treated rats showed negligible amounts of collagen fibers (X400). (H) Treatment with carcinogen revealed severe deposition of collagen fibers surrounding the hyperplastic nodules pseudolobules (x100). (I) Liver tissues of animals pretreated with Biobran before the carcinogen displayed slight deposition of collagen fibers around the central vein (x400). (J) Animals posttreated with Biobran showed moderate amounts of collagen fibers around the congested central (x400).

that Biobran exerts its apoptotic effect via a mitochondrial dependent pathway arises from our measurements of gene expression and protein levels. The effect of Biobran, both for pretreatment and posttreatment, up-regulated the relative gene expression and protein levels of p53 and Bax and down-regulated the anti-apoptotic Bcl-2 relative gene expression and protein level in liver tissues of untreated animals. These results are in accordance with other natural products that exert an apoptotic effect on hepatic cancer cells via activation of caspases, decreased levels

of Bcl-2, and slowed cell reproduction in the G2/M stage. These products include EFLDO extracted from the *Euphorbia* lunulata Bge [26], Amana edulis, Chinese herbal medicines [27], and Isoorientin from Gypsophila elegans [28]. Furthermore, Biobran treatment acted to increase the Bax/Bcl-2 ratio and caspase-3 expression when compared with the untreated carcinogen group. Many researchers have demonstrated that one of the important mechanisms for preventing hepatocarcinoma is increasing the Bax/Bcl-2 ratio [29–31]. Changes in these apoptotic molecules can cause disruption of the outer mitochondrial membrane and the release of cytochrome C that ultimately activates caspase-3, one of the key mediators of p53-induced apoptosis. Biobran's role in initiating mitochondrial mediated apoptosis has also been reported previously [9], where an increase in the levels of early and late apoptosis was observed in gastric cancer cells of rats co-treated with Biobran and the carcinogen MNNG. These results complement earlier studies that have shown that Biobran is a potent BRM that activates different immune cells that possess anti-tumor effects, such as DCs [10–12], NK cells [5,13–17], and human T and B cells [3]. The immunomodulatory effects of Biobran may represent an additional mechanism by which it exerts a protective effect against liver cancer.

In addition to studying Biobran's role in apoptosis, we sought to study its role in inflammation by measuring key molecular activity and by analyzing the histopathology of liver tissues. In the current study, the carcinogen (NDEA plus CCl_4) induced a marked elevation in the expression level of NF-κB/p65 in the cancerous liver cells, while treatment with Biobran markedly attenuated the NF-κB/p65 protein expression induced by the carcinogen. Similarly, while there was a marked increase in NF-κB/p65 immunoreactivity in the cytoplasm of hepatocytes of the rats that were only administered the carcinogen, treatment with Biobran markedly reduced the NF-κB/p65 immunoreactivity, with pretreatment revealing a greater degree of reduction than posttreatment. This inhibition of NF-κB activity might contribute to the hepatoprotective effects of Biobran against carcinogen-induced hepatocarcinogenesis. NF-κB has been demonstrated to be a key inflammatory factor in tumorigenesis [32] and has been shown to be up-regulated both in human hepatocarcinoma [33] and in experimental animals [34]. In unstimulated cells, NF-κB binds to IκB, the NF-κB inhibitor, in the cytoplasm. After IκB undergoes phosphorylation and degradation, NF-κB is released and activated [35,36], translocating to the nucleus where it stimulates the transcription of many of the key genes responsible for inflammation, proliferation, invasion, metastasis, and inhibition of apoptosis [36,37]. Several researchers have revealed that constitutive activation of NF-κB is accompanied by hepatocarcinogenesis [33,38], and Ueno et al. [39] have noted an increase of NF-κB expression in the liver tissues of rats that received the carcinogen. It has also been reported that an increase in the expression of NF-κB in NDEA-induced hepatocarcinogenic rats is correlated with more aggressive lesions and tumor growth [40]. The inhibition of NF-κB activity has been shown to significantly reduce the proliferation and invasion of the Hep3B cell line, demonstrating that the inhibition of NF-κB may be a potential therapeutic target for HCC [41].

In the current study, we also showed that the carcinogen reduced the IκB-α–relative gene expression in cancerous liver cells, while treatment with Biobran markedly inhibited the degradation of IκB-α induced by the carcinogen. Furthermore, carcinogen exposure led to an increase in the phosphorylation of IκB-α, consistent with the increase in the NF-κB/p65 protein level, the active form of NF-κB. Treatment with Biobran returned IκB-α levels closer to the control levels. It has previously been reported that the increase of total IκB-α but the decrease of IκB-α phosphorylation is an important intervention target for inhibiting tumor cell metastasis [42]. Our study indicates that Biobran inhibited the degradation of IκB-α induced by the carcinogen and promoted NF-κB in the resting state, which might contribute to its protective effects against carcinogen-induced hepatocarcinogenesis.

Finally, we studied the histopathological changes in liver cells in the presence or absence of Biobran. The carcinogen induced different proliferative and preneoplastic lesions in the livers of rats. Treatment with carcinogen caused a loss of architecture in liver cancer cells as well as steatosis, while treatment with Biobran decreased the appearance of steatosis and increased the appearance of inflammatory infiltrates such as lymphocytes, both for pretreatment and posttreatment groups. Furthermore, pretreatment with Biobran preserved the hepatic architecture with minimal mitosis and nuclear changes as well as minimal inflammation and absence of collagen deposition. These results support the role of Biobran as an antineoplatic agent. These results are in correspondence with previous results showing that Biobran possesses strong anticancer effects against several neoplasms, including solid Ehrlich carcinoma [5,43], glandular stomach carcinogenesis in rats [9], neuroblastoma in mice [6], and metastatic hemangiopericytoma [44].

5. Conclusions

We conclude that Biobran has the ability to inhibit hepatocarcinogenesis induced by a carcinogen (NDEA plus CCl_4) via induction of apoptosis and inhibition of inflammation and cancer cell proliferation. Molecular studies of the liver tissues demonstrated that Biobran reversed the carcinogen induced suppression of IkappaB-alpha (IκB-α) gene expression; downregulated the expression of nuclear factor kappa-B (NF-κB/p65) and Bcl-2; upregulated the relative gene expression and protein levels of p53, Bax, and caspase-3; and increased nuclear DNA fragmentation-based apoptosis in liver tissues. Biobran may be a promising chemopreventive and chemotherapeutic agent for liver carcinogenesis.

Funding

Partial support was provided by Daiwa Pharmaceutical Co., Ltd., Tokyo, Japan.

Declaration of Competing Interest

Partial support was provided by Daiwa Pharmaceutical Co., Ltd., Tokyo, Japan.

References

[1] World Cancer Research Fund, Liver Cancer Statistics, (2019) https://www.wcrf.org/dietandcancer/cancer-trends/liver-cancer-statistics.
[2] F. Bray, J. Ferlay, I. Soerjomataram, R.L. Siegel, T.A. Torre, A. Jemal, Global Cancer Statistics, Global cancer statistics 2018: GLOBOCAN estimates of incidence and mortality worldwide for 36 cancers in 185 countries, CA Cancer J. Clin. 68 (6) (2018) 394–424, https://doi.org/10.3322/caac.21492 The online GLOBOCAN 2018 database is accessible at http://gco.iarc.fr/ , as part of IARC's Global Cancer Observatory.
[3] M. Ghoneum, Anti-HIV activity in vitro of MGN-3, an activated arabinoxylan from rice bran, Biochem. Biophys. Res. Commun. 243 (1998) 25–29.
[4] M.H. Bang, T. Van Riep, T.N.T. Thinh, et al., Arabinoxylan rice bran (MGN-3) enhances the effects of interventional therapies for the treatment of hepatocellular carcinoma: a three-year randomized clinical trial, Anticancer Res. 30 (2010) 5145–5151.
[5] N.K. Badr El-Din, E. Noaman, M. Ghoneum M, In vivo tumor inhibitory effects of nutritional rice bran supplement MGN-3/Biobran on Ehrlich Carcinoma-Bearing mice, Nutr. Cancer 60 (2008) 235–244.
[6] A. Pérez-Martínez, J. Valentín, L. Fernández, et al., Arabinoxylan rice bran (MGN-3/Biobran) enhances natural killer cell-mediated cytotoxicity against neuroblastoma in vitro and in vivo, Cytotherapy 17 (2015) 601–612.
[7] N.K. Badr El-Din, S.K. Areida, K.O. Ahmed, M. Ghoneum, Arabinoxylan rice bran (MGN-3/Biobran) enhances radiotherapy in animals bearing Ehrlich ascites carcinoma, J. Radiat. Res. 60 (2019) 747–758.
[8] N.K. Badr El-Din, D.A. Ali, M. Alaa El-Dein, M. Ghoneum, Enhancing the apoptotic effect of a low dose of paclitaxel on tumor cells in mice by arabinoxylan rice bran (MGN-3/Biobran), Nutr. Cancer 68 (2016) 1010–1020.
[9] N.K. Badr El-Din, S.M. Abdel Fattah, D. Pan, L. Tolentino, M. Ghoneum, Chemopreventive activity of MGN-3/Biobran against chemical induction of glandular stomach carcinogenesis in rats and its apoptotic effect in gastric cancer cells, Integr. Cancer Ther. 15 (2016) NP26–NP34.
[10] D. Cholujova, J. Jakubikova, J. Sedlak, Biobran-augmented maturation of human monocyte-derived dendritic cells, Neoplasma 56 (2009) 89–95.
[11] M. Ghoneum, S. Agrawal, Activation of human monocyte-derived dendritic cells in

vitro by the biological response modifier arabinoxylan rice bran (MGN-3/Biobran), Int. J. Immunopathol. Pharmacol. 24 (2011) 941–948.
[12] M. Ghoneum, S. Agrawal, MGN-3/biobran enhances generation of cytotoxic CD8 + T cells via upregulation of dec-205 expression on dendritic cells, Int. J. Immunopathol. Pharmacol. 27 (2014) 523–530.
[13] M. Ghoneum, Enhancement of human natural killer cell activity by modified arabinoxylan from rice bran (MGN-3), Int. J. Immunother. 14 (1998) 89–99.
[14] M. Ghoneum, A. Jewett, Production of tumor necrosis factor-alpha and interferon-gamma from human peripheral blood lymphocytes by MGN-3, a modified arabinoxylan from rice bran, and its synergy with interleukin-2 in vitro, Cancer Detect. Prev. 24 (2000) 314–324.
[15] M. Ghoneum, S. Abedi, Enhancement of natural killer cell activity of aged mice by modified arabinoxylan rice bran (MGN-3/Biobran), J. Pharm. Pharmacol. 56 (2004) 1581–1588.
[16] M. Ghoneum, J. Brown, NK immunorestoration of cancer patients by MGN-3, a modified arabinoxylan rice bran (study of 32 patients followed for up to 4 years), in: R. Klatz, R. Goldman R (Eds.), Anti-Aging Medical Therapeutics, Vol. III Health Quest Publications, Marina del Rey, CA, 1999, pp. 217–226.
[17] D. Cholujova, J. Jakubikova, B. Czako, et al., MGN-3 arabinoxylan rice bran modulates innate immunity in multiple myeloma patients, Cancer Immunol. Immunother. 62 (2013) 437–445.
[18] M. Ghoneum, M. Matsuura, Augmentation of macrophage phagocytosis by modified arabinoxylan rice bran (MGN-3/biobran), Int. J. Immunopathol. Pharmacol. 17 (2004) 283–292.
[19] N.K. Badr El-Din, D.A. Ali, R.M. Othman, Inhibition of experimental carcinogenesis by the bioactive natural product Biobran, J. Plant Protect. Pathol. 7 (2016) 85–91.
[20] S. Sundaresan, P. Subramanian, S-Allylcysteine inhibits circulatory lipid peroxidation and promotes antioxidants in N-nitrosodiethylamine-induced carcinogenesis, Pol. J. Pharmacol. 55 (2003) 37-34.
[21] P.J. Masson, AFIP modification, J. Tech. Methods 12 (1929) 75–90.
[22] C. Riccardi, I. Nicoletti, Analysis of apoptosis by propidium iodide staining and flow cytometry, Nat. Protoc. 1 (2006) 1458–1461.
[23] K.J. Livak, T.D. Schmittgen, Analysis of relative gene expression data using real-time quantitative PCR and the 2(-Delta Delta C(T)) Method, Methods 25 (2001) 402–408.
[24] M. Herrmann, H.M. Lorenz, R. Voll, M. Grunke, W. Woith, J.R. Kalden, A rapid and simple method for the isolation of apoptotic DNA fragments, Nucleic Acids Res. 22 (1994) 5506–5507.
[25] M. Ghoneum, S. Gollapudi, Modified arabinoxylan rice bran (MGN-3/Biobran) sensitizes human T cell leukemia cells to death receptor (CD95)-induced apoptosis, Cancer Lett. 201 (2003) 41–49.
[26] Y.B. Qu, Z.X. Liao, C. Liu, X.Z. Wang, J. Zhang, EFLDO induces apoptosis in hepatic cancer cells by caspase activation in vitro and suppresses tumor growth in vivo, Biomed. Pharmacother. 100 (2018) 407–416.
[27] Y. Fan, X. Hou, P. Guo, X. Lv, L. Zhao, H. Wang, L. Zhou, Y. Feng, Extraction of Amana edulis induces liver cancer apoptosis, Evid. Complement. Alternat. Med. 20 (2018) 3927075.
[28] X. Lin, J. Wei, Y. Chen, P. He, J. Lin, S. Tan, J. Nie, S. Lu, M. He, Z. Lu, Q. Huang, Isoorientin from Gypsophila elegans induces apoptosis in liver cancer cells via mitochondrial-mediated pathway, J. Ethnopharmacol. 187 (2016) 187–194.
[29] Y. Ji, C. Ji, L. Yue, H. Xu, Saponins isolated from Asparagus induce apoptosis in human hepatoma cell line HepG2 through a mitochondrial-mediated pathway, Curr. Oncol. 19 (Suppl. 2) (2012) eS1–eS9.
[30] U. Das, S. Biswas, S. Chattopadhyay, A. Chakraborty, R.D. Sharma, A. Banerji, S. Dey, Radiosensitizing effect of ellagic acid on growth of Hepatocellular carcinoma cells: an in vitro study, Sci. Rep. 7 (2017) 14043.
[31] N. Abdel-Hamid, M.F. El-Azab, Y.M. Moustafa, Macrolide antibiotics differentially influence human HepG2 cytotoxicity and modulate intrinsic/extrinsic apoptotic pathways in rat hepatocellular carcinoma model, Naunyn Schmiedebergs Arch. Pharmacol. 390 (2017) 379–395.
[32] X. Dolcet, D. Llobet, J. Pallares, X. Matias-Guiu, NF-kB in development and progression of human cancer, Virchows Arch. 446 (2005) 475–482.
[33] D.I. Tai, S.L. Tsai, Y.H. Chang, S.N. Huang, T.C. Chen, K.S.S. Chang, Y.F. Liaw, Constitutive activation of nuclear factor kB in hepatocellular carcinoma, Cancer. 89 (2000) 2274–2281.
[34] X. Zhang, S. Liu, T. Hu, S. Liu, Y. He, S. Sun, Up-regulated microRNA-143 transcribed by nuclear factor kappa B enhances hepatocarcinoma metastasis by repressing fibronectin expression, Hepatology 50 (2009) 490–499.
[35] R.F. Schwabe, T. Luedde, Apoptosis and necroptosis in the liver: a matter of life and death, Nat. Rev. Gastroenterol. Hepatol. 15 (2018) 738–752.
[36] A.C. Bharti, B.B. Aggarwal, Nuclear factor-kappa B and cancer: its role in prevention and therapy, Biochem. Pharmacol. 64 (2002) 883–888.
[37] B.B. Aggarwal, A. Bhardwaj, R.S. Aggarwal, N.P. Seeram, S. Shishodia, Y. Takada, Role of resveratrol in prevention and therapy of cancer: preclinical and clinical studies, Anticancer Res. 24 (2004) 2783–2840.
[38] P. Liu, E. Kimmoun, A. Legrand, A. Sauvanet, C. Degott, B. Lardeux, D. Bernuau, Activation of NF-kappa B, AP-1 and STAT transcription factors is a frequent and early event in human hepatocellular carcinomas, J. Hepatol. 37 (2002) 63–71.
[39] S. Ueno, D. Aoki, F. Kubo, K. Hiwatashi, K. Matsushita, T. Oyama, I. Maruyama, T. Aikou, Roxithromycin inhibits constitutive activation of nuclear factor κB by diminishing oxidative stress in a rat model of hepatocellular carcinoma, Clin. Cancer Res. 11 (2005) 5645–5650.
[40] P. Subramanian, D. Arul, Attenuation of NDEA induced hepatocarcinogenesis by naringenin in rats, Cell Biochem. Funct. 31 (2012) 511–517.
[41] J.M. Wu, H. Sheng, R. Saxena, N.J. Skill, P. Bhat-Nakshatri, M. Yu, H. Nakshatri, M.A. Maluccio, NF-kappaB inhibition in human hepatocellular carcinoma and its potential as adjunct to sorafenib based therapy, Cancer Lett. 278 (2009) 145–155.
[42] K. Guo, N.X. Kang, Y. Li, L. Sun, L. Gan, F.J. Cui, M.D. Gao, K.Y. Liu, Regulation of HSP27 on NF-kappaB pathway activation may be involved in metastatic hepatocellular carcinoma cells apoptosis, BMC Cancer 9 (2009) 100.
[43] E. Noaman, N.K. Badr El-Din, M.A. Bibars, A.A. Abou Mossallam, M. Ghoneum, Antioxidant potential by arabinoxylan rice bran, MGN-3/biobran, represents a mechanism for its oncostatic effect against murine solid Ehrlich carcinoma, Cancer Lett. 268 (2008) 348–359.
[44] J. Markus, A. Miller, M. Smith, I. Orengo, Metastatic hemangiopericytoma of the skin treated with wide local excision and MGN-3, Dermatol. Surg. 32 (2006) 145–147.